Title
Materials Engineering by Ameloblasts

Journal
Journal of Dental Research, 94(6)

ISSN
1045-4411

Author
Habelitz, S

Publication Date
2015-06-01

DOI
10.1177/0022034515577963

Peer reviewed

Journal of Dental Research
2015, Vol. 94(6) 759–767

DOI: 10.1177/0022034515577963
jdr.sagepub.com

Materials Engineering by Ameloblasts

S. Habelitz[1]

Abstract

Enamel is unique. It is the only epithelial-derived mineralized tissue in mammals and has a distinct micro- and nanostructure with nanofibrous apatite crystals as building blocks. It is synthesized by a highly specialized cell, the ameloblast, which secretes matrix proteins with little homology to any other known amino acid sequence, but which is composed of a primary structure that makes it competent to self-assemble and control apatite crystal growth at the nanometer scale. The end-product of ameloblast activity is a marvel of structural engineering: a material optimized to provide the tooth with maximum biting force, withstanding millions of cycles of loads without catastrophic failure, while also protecting the dental pulp from bacterial attack. This review attempts to bring into context the mechanical behavior of enamel with the developmental process of amelogenesis and structural development, since they are linked to tissue function, and the importance of controlling calcium phosphate mineralization at the nanometer scale. The origins of apatite nanofibers, the development of a stiffness gradient, and the biological processes responsible for the synthesis of a hard and fracture-resistant dental tissue are discussed with reference to the evolution of enamel from a fibrous composite to a complex, tough, and damage-tolerant coating on dentin.

Keywords: enamel, structure, evolution, properties, gradient, enamel matrix

Introduction to the Evolution of Enamel Structure

Biomineralization, mineralization of tissues or mineralization controlled by biology, is a concept that developed about 570 million years ago (Mann 2001). The ability of living organisms to deposit mineral provided an evolutionary advantage by generating protective (shells, spicules) and weight-bearing (exo- and endoskeletons) structures. This new ability heavily expanded animal diversity and the presence of higher organisms on the planet. Furthermore, mineralization produced tissues with increased hardness, and stiffness allowed for consumption of food resources previously not accessible.

Bony structures can function for mastication and may have been an early evolutionary attempt to generate dental structures (Smith and Coates 1998), but this level of hardness is not sufficient to avoid significant abrasion of the tissue over time (Table). There are 2 general theories for the evolutionary origin of teeth (Fraser et al. 2010). There is evidence that, during the late Cambrian period, 500 million years ago, dermal structures mineralized superficially (dermal armor), and ectodermal invagination into the oral cavity transformed these structures into the first masticatory tissues (Soukup et al. 2008). In another model, mineralized structures developed in possibly the endothelium of the pharynx and gradually moved into the oral cavity to function as teeth (Smith and Coates 1998). Both concepts share the biological event that defines the genesis of a tooth. The reciprocal interactions of migratory mesenchyme-derived neural crest cells with epithelial cells induced the differentiation of 2 highly specialized cell types: the odontoblast and the ameloblast (Thesleff and Hurmerinta 1981). Once fully differentiated, the 2 cell types gradually migrate away from each other while secreting matrices that self-assemble and control mineral nucleation and growth (Nanci and Ten Cate 2013).

Enameloid is the term for the mineralized layer that covers teeth in chondrichthyans (sharks and rays), actinopterygians (bony fish), and early larval stages of caudate amphibians, e.g., newts and salamanders (Davit-Beal et al. 2007). Enameloid develops from dental epithelial and odontoblast activity, and it is composed, at least initially, of matrices containing predominantly collagen (Sasagawa et al. 2009). This suggests that enameloid may be associated with dentin formation and is thus different from enamel (Davit-Beal et al. 2007; Assaraf-Weill et al. 2014). While it is not fully understood if enameloid and enamel are related evolutionarily, it has been shown that several species (newts, salamanders, some fish) that produce enameloid structures also have a mineral coating that appears to be enamel, since it is synthesized by ameloblasts (Satchell et al. 2002; Davit-Beal et al. 2007; Diekwisch et al. 2009). These layers reveal structural and compositional characteristics of enamel, since their matrices are composed of tuftelins, enamelins, amelogenins, and enamel-specific enzymes (Diekwisch et al. 2002; Satchell et al. 2002). The tooth surface of

[1]Preventive and Restorative Dental Sciences, University of California, San Francisco, CA, USA

Corresponding Author:
S. Habelitz, 707 Parnassus Ave. D-3211, San Francisco, CA 94143-0758, USA.
Email: Stefan.habelitz@ucsf.edu

Table. Properties of Mineralized Tissues.

	Hardness (nanoindentation), GPa	Modulus (nanoindentation), GPa	Strength (bending), MPa	Toughness K_{1c} $MPam^{1/2}$
Enamel	2.5 – 6.0 (a, b)	55 – 120 (a, b)	80 – 150 (c)	1.0 – 4.0 (d, e)
Dentin	0.5 – 0.8 (f)	15 – 22 (f)	60 – 200 (g)	1.5 – 3.0 (h)
Bone (compact)	0.6 – 0.7 (i)	13 – 21 (l, j)	80 – 300 (j)	2.0 – 7.7 (j, k)
Aprismatic enamel	3.0 – 3.3 (l)	31 – 42 (m)	–	*0.2 – 0.3 (m) = 50% prismatic enamel*
Enameloid	3.2 – 3.5 (n)	69 – 73 (n)	–	–
Nacre	2.5 – 3.0 (o)	60 – 75 (o)	200 – 250 (o)	8 – 12 (o)

Italics indicate that the method used in that experiment was different from others in the list.
References: (a) Cuy et al. 2002; (b) Habelitz et al. 2001; (c) Bechtle, Fett, et al. 2010; (d) Bechtle, Habelitz, et al. 2010; (e) Bajaj and Arola 2009b; (f) Marshall et al. 2001; (g) Kinney et al. 2003; (h) Imbeni et al. 2005; (i) Feng et al. 2012; (j) Currey 2002; (k) Nalla et al. 2005; (l) Enax et al. 2013; (m) Yilmaz et al. 2014; (n) Whitenack et al. 2010; (o) Meyers et al. 2011.

the modern-day shark is shown as an example in Fig. 1. It is composed of a triple-layer structure with the outermost "shiny" layer matching the characteristics of enamel, whereas the underlying layers contain collagen and thus constitute enameloid (Gillis and Donoghue 2007). Similar to enamel, enameloid is primarily built from apatite nanofibers, which vary in diameter between 30 and 100 nm (Fig. 1A, B). In contrast to mammalian enamel, enameloid does not contain enamel rods. Instead, apatite fibers are packed into narrow domains of parallel fibers, and fibers are shorter and often bent and curved (Fig. 1A, B).

The surface coating of reptile teeth is termed "enamel," since it is produced by the enamel organ and ameloblasts (Satchell et al. 2002; Diekwisch et al. 2009). As an example of its ultrastructure, crocodile enamel is shown in Figure 1C and D. It is composed of mineral nanostructures, predominantly fibers with less defined crystal surfaces compared with those of shark or mammalian enamel. The crystals are aligned in parallel, with their long axes perpendicular to the tooth surface. Enamel in amphibians and reptiles is therefore denoted "parallel crystallite enamel" (Sander 2000). It is very thin, measuring from a few micrometers in frog teeth to about 200 μm in large lizards (Diekwisch et al. 2002). Reptile enamel is considered an evolutionary ancestor of mammalian enamel and is used as a reference to "early or primitive" enamel in this review.

The advent of prismatic enamel, which is enamel composed of micrometer-sized rod-like structures, was a significant step in evolution and led to a change from the canine-like morphology of teeth (zyphodonts) to the dentition of heterodonts, with a large diversity of tooth types and shapes optimized to function (Sahni 1987). While ameloblasts migrate away from the mineralizing front at a 90° angle and are thus in parallel to the alignment of apatite fibers in primitive aprismatic enamel, in mammalian enamel, the angle between the rod axis and polarized ameloblasts is approximately 60° (Hanaizumi et al. 1994; Sander 2000) (Fig. 2A, B). The angulation led to a curved apical end of the polarized ameloblast and the formation of a true extension, the "Tomes' process" (Smith and Coates 1998). Enamel matrix proteins are secreted through the Tomes' process and orchestrate the mineralization process that produces apatite nanofibers and their alignment. The Tomes' process remains connected to the matrix and the enamel rod through the entire secretory stage of amelogenesis. The migration pathway of ameloblasts is therefore directly associated with the rod orientation. An enamel rod or prism measures, on average, 5 μm in diameter and penetrates most of the enamel thickness, since it extends from an aprismatic zone close to the dentin-enamel junction (DEJ) nearly to the surface of the tooth. A thin layer composed of aligned apatite crystallites, which differs in orientation from the intrarod crystals surrounding each rod, is termed "interrod enamel" (Fig. 1E–J). The existence of enamel rods is intrinsically intertwined with the occurrence of interrod enamel. Both play a critical role in the mechanical and fracture behavior of enamel, as discussed below. Interestingly, enamel rods are absent and no longer develop in mice that lack amelogenin (Gibson et al. 2001) (Fig. 1K, L). Instead, the enamel of $Amelx^{-/-}$ mice has appearance similar to that of the prismless enamel of reptiles (Fig. 1C, D), suggesting that ameloblasts switch back to an evolutionarily older enamel structure once amelogenin is absent from the matrix (Fig. 1K, L).

Developmental Strategies to Optimize Enamel Properties for Tooth Function

Aligned Apatite Nanofibers

Mineral fibers that crystallize in enamel are nanometer-sized, which fits well with a concept introduced by Griffith (1921). In brittle materials, the ultimate strength is a function of the dimension of the largest flaw in the material. Since flaws are restricted to the dimension of the grain in a polycrystalline material, materials composed of nanocrystals usually exhibit increased strength. In the case of carbon nanotubes (diameter, 30 nm), the tensile strength can reach 100 GPa and exceeds the strength of an already strong 10 μm Kevlar polymer fiber by 30 times (Chang et al. 2010). Hence, at least according to the Griffith model, the effort by the ameloblast to control crystal growth and to produce 50-nm-wide fibers appears fully justified. The surprising part to an engineer, however, is the orientation for such nanofibers, since fiber reinforcement works best when tensile stresses are applied parallel to the fibril axis and cracks are initiated perpendicular to that axis. On a simplified view, this appears to be the opposite in dental enamel, since one may expect cracks to penetrate enamel and cause

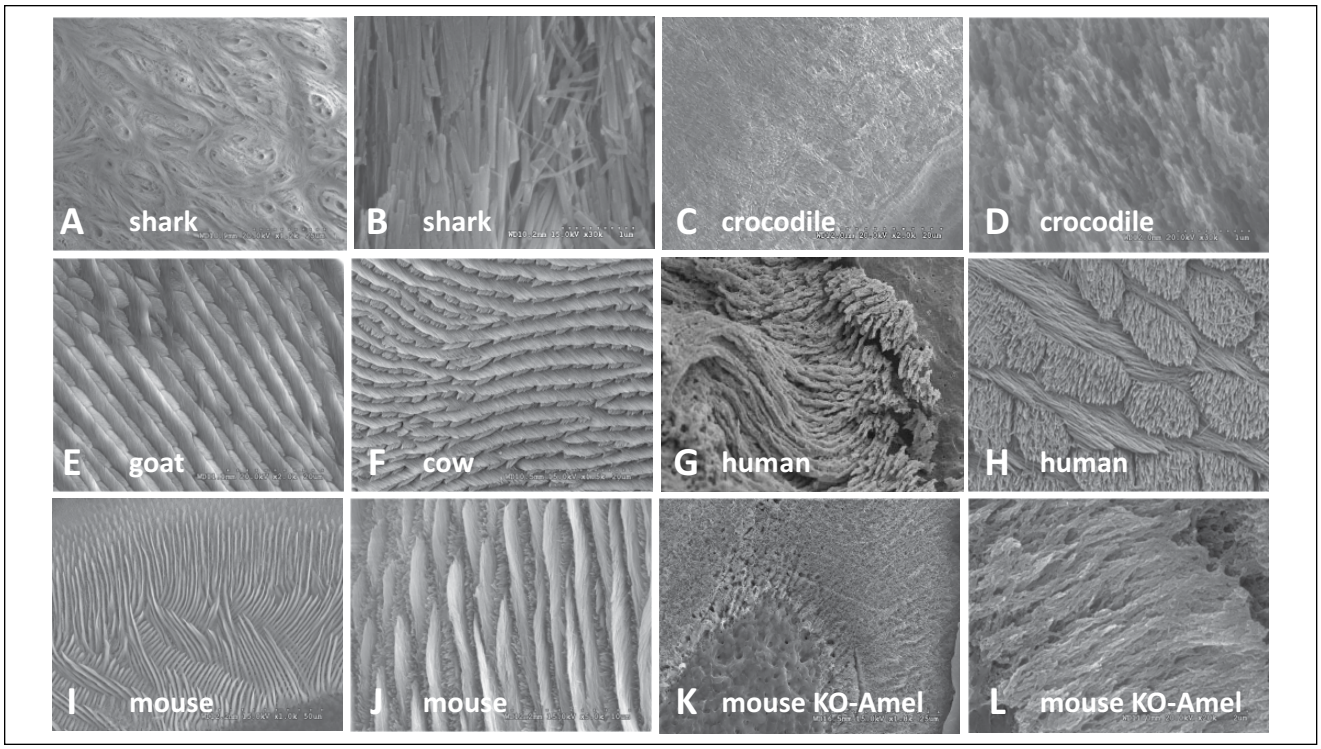

Figure 1. Scanning electron microscope images of the end-product of ameloblast activity, the mineralized enamel, from different vertebrate animals. Enamel from the zebra shark (*Stegostoma fasciatum*), crocodile (*Crocodylus acutus*), goat, and mouse is shown at low magnification (from 2,000 to 4,000X) to provide an overview of microstructure, adjacent to a higher-magnification micrograph (from 25,000 to 50,000X) to reveal organization of apatite nanofibers. (**A, B**) Enameloid from the zebra shark: tangled fiber enameloid (A) and parallel-fiber enameloid (B). (**C, D**) Oriented crystallite enamel of the crocodile. (**E, F**) Rod-interrod arrangement in goat (E) and bovine (F) enamel. (**G, H**) Prismatic enamel in a human, with a wavy pattern near the dentin-enamel junction (DEJ) (G) and rod-interrod structure in decussated enamel (H) (modified from Bechtle et al. 2010). (**I, J**) Rod-interrod distribution in wild-type murine enamel. (**K, L**) Enamel microstructure from amelogenin knock-out mice ($Amelx^{-/-}$), illustrating structural similarities to reptile enamel in C and D. Specimens were polished and etched with 10% HCl for 10 to 30 s prior to being imaged; sample H was etched for 72 h.

catastrophic fracture or chipping. In fact, analysis of recent mechanical data on primitive enamel confirmed such concerns (Yilmaz et al. 2014). Aprismatic enamel from a lizard, with apatite crystal alignment similar to that observed in a crocodile (Fig. 1C, D), was examined in micro-cantilever bending tests. Cracks readily followed the axes of oriented crystallites, reducing toughness values to about half to one-third of the values reported for prismatic enamel in humans (Table) (Bechtle, Habelitz, et al. 2010; Yilmaz et al. 2014).

Mastication works best when stiffness and hardness of the tissue are highest. Hence, maximizing the mineral content is a main driving force in the evolution of the tooth's surface coating. A secondary function, however, may have played an equal role in the preference for aligned nanofibers for this mineral coating vs other morphologies of crystals. Apatite is soluble in mild and cariogenic acids, but the progress of a caries lesion through enamel is severely limited, since bacteria do not flourish on enamel without exogenous carbohydrates. This is well-illustrated by the sudden increase in size of caries lesions once the bacteria have penetrated the DEJ and have spread extensively in dentin (Zheng et al. 2003). The occlusal surface layer of human enamel is actually prism-less, and a zone of 5 to 20 μm is composed of well-aligned apatite nanofibers, most likely devoid of any protein (Nanci and Ten Cate 2013).

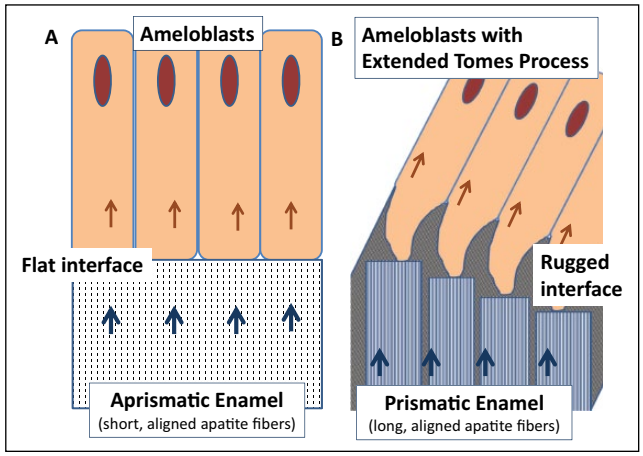

Figure 2. Schematic representations of ameloblast configuration and morphology on different types of enamel during the secretory stage of amelogenesis. (**A**) In the aprismatic enamel of reptiles, polarized ameloblasts are oriented in parallel with the orientation of short apatite fibers, creating a flat interface between cells and the mineralization front. (**B**) In the prismatic enamel of mammals, ameloblasts are oriented in an angle toward the enamel rod. The angulation leads to an extended Tomes' process, with matrix being secreted from its distal end and through the lateral portions, forming a rugged interface between ameloblasts and the mineralization front.

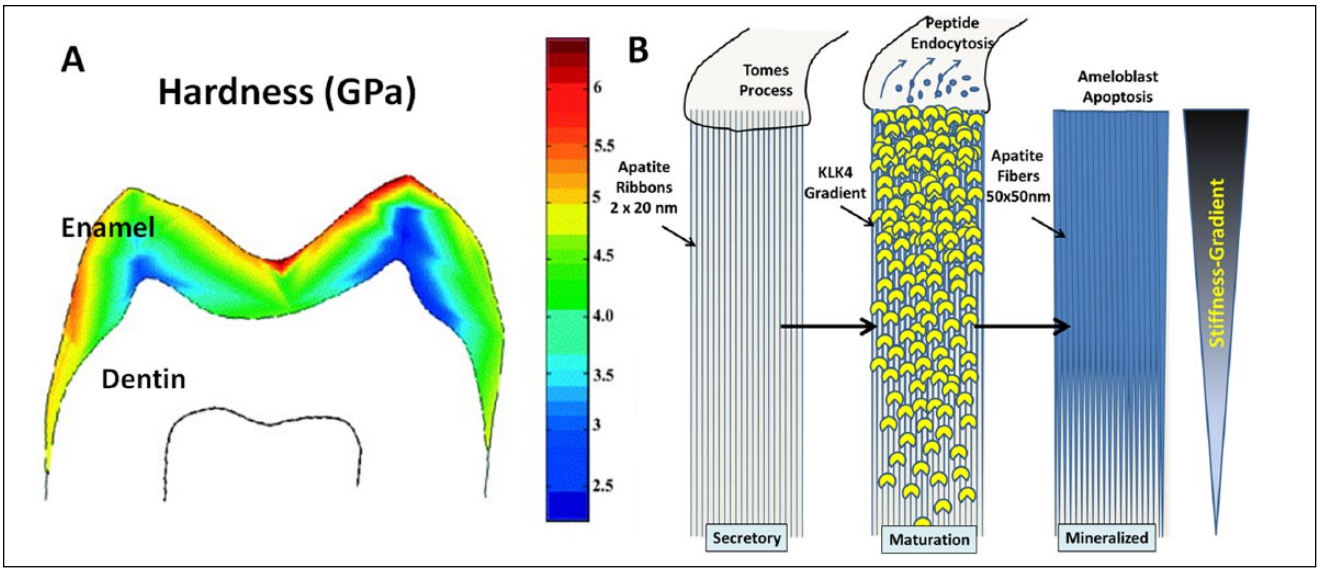

Figure 3. Relationship between hardness gradient and protease activity during enamel maturation. (**A**) Map of hardness values obtained by nanoindentation across sagittal section of human molar (modified from Cuy et al. 2001). The hardness decreases from about 6 GPa at the occlusal contacts to about 2.5 GPa at the dentin-enamel junction (DEJ), as indicated by the color scheme. (**B**) Illustration of the development of individual crystallites in an enamel rod during amelogenesis. Secretory stage shows apatite crystallites 2–3 nm thick, 10–20 nm wide. These nanoribbons most likely run continuously from the DEJ to close to the occlusal surface of the enamel. At the beginning of the maturation stage, the enzyme KLK-4 is secreted into the extracellular space through the Tomes' process. A gradient of active enzyme develops as KLK-4 diffuses into the lumen of the enamel rod toward the DEJ. Removal of protein allows for lateral extension of apatite crystals, which are now fibrous and measure about 50 nm in diameter. The mineralized enamel rod is the final product of the activity of one ameloblast. It is composed of a gradient of mineral content with possibly protein-free apatite at the occlusal zone, which is aprismatic, and increasing organic residue toward the DEJ, resulting in a gradient of stiffness and hardness.

Generating a dense mineral layer on top of the collagen-rich dentin not only provides increased hardness, but also protects the underlying collagenous tissues from hydrolysis by bacterial attack. It is this high degree of fiber alignment that allows for a high-density mineralized tissue with minimal porosity to protect from caries progression. By analogy, incorrect or disrupted mineralization of enamel, as a result of genetic mutations (amelogenesis imperfecta) or due to fluorosis, elevates the incidence of caries, since the increased porosity in enamel accelerates the demineralization process (Lyaruu et al. 2014). By analogy, crystallites in enameloid of revolving teeth, as in sharks (Fig. 1A, B), are not as densely packed and contain pores. Longevity is not as critical for revolving teeth, since they are replaced continuously and frequently.

Stiffness Gradient

The primary function of enamel is to provide a hard surface on a masticatory structure, e.g., dentin, to allow for the breakdown of food bolus. The hardness and stiffness of enamel are maximized when the mineral content of enamel reaches its maximum, e.g., 100% apatite. The shortcoming of such an approach is that a pure apatite structure is severely brittle. Toughness of pure apatite may be lower than that of glass, and enamel that was depleted of its organic phase has been reported to exhibit poor mechanical performance (White et al. 2001; Baldassarri et al. 2008).

Geological apatite single crystals (E = 100–120 GPa) (Katz and Ukraincik 1971) have an elastic modulus and hardness about 5 to 6 times higher than those of dentin or bone (E = 15–20 GPa) (Table). Hence, any elastic deformation of the tooth during mastication will induce interfacial stresses at the DEJ, since dentin tries to deform to a larger extent than does enamel. An elegant solution to reduce this problem is the generation of a property gradient in enamel—an approach that materials engineers have recognized and have attempted to mimic in the design of dental crowns (Lawn et al. 2002). When hardness is sampled across the thickness of a human molar by nanoindentation, properties decrease from the occlusal surface toward the DEJ (Cuy et al. 2002; He and Swain 2009). At occlusal contacts, hardness values of about 6 GPa are reached, indicating that this layer might be pure apatite mineral and protein-free (Fig. 3A), while near the DEJ, hardness is as low as 2.5 to 3 GPa (Cuy et al. 2002). Other nanoindentation studies also examined the elastic modulus of enamel and observed that the modulus decreased from about 90 GPa at the outer enamel to values between 75 and 60 GPa at the inner third of enamel (He and Swain 2009; Jeng et al. 2011). Both the hardness and modulus gradients in enamel suggest that proteases extensively remove enamel proteins at the enamel surface, while more residual protein remains at a zone close to the DEJ. Spectroscopic analysis further showed an increased amount of amide content in the inner enamel, with no clear indication of organic components at the surface (He and Swain 2009). A mineral gradient has been determined in deciduous and permanent human teeth (Wong et al. 2004; Sa et al. 2014) and, to a small extent, in the thin enamel layer of crocodile teeth (200 μm). This indicates that the strategy of integrating the 2

dissimilar tissues by a graded structure may have been adapted fairly early in evolution (Enax et al. 2013).

In mineralized collagenous tissues, a relationship between mineral content and hardness and stiffness is clearly established and illustrated in a wide range of properties in different tissues, as well as in specimens that have been partially demineralized (Fratzl 2008). By analogy, the gradient in stiffness and hardness of enamel is directly related to the mineral-to-protein ratio across the thickness of enamel. Therefore, the matrix protein removal process must be associated with the tissue's ability to obtain graded properties. The matrix of enamel is secreted and immediately processed by a metallomatrix protease, MMP-20, but a very limited amount of matrix is removed at this stage (Bartlett et al. 2006). Apatite crystals develop early during the secretory stage of ameloblasts and, initially, are only about 2 to 3 nm thick and 10 to 20 nm wide (Fig. 3B). In coordination with the movement of ameloblasts, proteins are secreted into the extracellular space underneath a tightly connected cell layer. While the cells migrate away from the mineralizing front, the fine ribbons of apatite grow in length. Current imaging methods do not allow for the exact determination of the full length of enamel crystallites, but fibers extending to lengths of tens of micrometers have been shown (Daculsi and Kerebel 1978; Nanci and Ten Cate 2013). Many have also hypothesized that these apatite ribbons span the entire thickness of the enamel layer by the end of the secretory stage, possibly as one extremely fine, long, single crystal. The thickness of the early apatite ribbons deposited at the DEJ increases somewhat to about 10 nm, but more than 60% of the mineral in enamel forms after the secretory stage (Simmer et al. 2010). This is mainly due to the release of a second enamel enzyme at the beginning of the maturation stage (Simmer and Hu 2002). Serine protease, kallikrein-4 (KLK-4), heavily hydrolyzes the enamel matrix and ingestion and removal of the cleavage products by ameloblasts, allowing for lateral growth of apatite ribbons to an average diameter of around 50 nm. Since serine proteases are produced and secreted at the enamel surface, a gradient develops as proteases diffuse into the bulk of the enamel matrix. KLK-4 penetration into the depth of the developing enamel matrix is a function of the diffusion rate (Fig. 3B). In addition, activation of KLK-4 is most likely executed by a cysteine aminopeptidase, which is primarily expressed during the maturation stage and thus needs to diffuse from the surface into the developing matrix, possibly further augmenting the gradient profile active enzyme distribution throughout the volume of mineralizing enamel (Tye et al. 2009). Enzyme activity decreases with time spent in the matrix. Thus, highly active and concentrated enzymes are primarily present at the ameloblast-enamel matrix interface, and protease concentration and activity reduce toward the DEJ. As a consequence, a superficial zone in enamel appears to be depleted of any organic phases, while residual protein remains to a larger extent in the inner enamel and at the DEJ (He and Swain 2009; Sa et al. 2014). The result is a material with a stiffness gradient that aids in improving the integration of 2 dissimilar mineralized tissues: enamel and dentin.

Decussating and Interrod Enamel

As described above, in contrast to primitive enamel, ameloblasts retreat from the mineralizing front in an angle. The pathway of the polarized ameloblast is offset from the parallel alignment with the enamel rod, and the cell body migrates away from the mineralizing front, maintaining an angular tilt of about 30° in relation to the rod direction. In prismatic enamel, the shape of the ameloblast has evolved to become an actual cell protrusion of the Tomes' process developed. In the classic schematic relationship between the Tomes' process and the enamel rod, the interface between the 2 has the shape of a "picket fence," as described by Boyde (1967) (Fig. 2B).

The origin of the 2 different compartments, rod and interrod, of enamel crystals derives from an asymmetric deposition of matrix protein, which occurs at 2 distinct secretory sites (Nanci et al. 1996). Enamel matrix is exocytosed not only at the distal end of the Tomes' process (distTP) but also through the proximal endings of the processes (proxTP). The latter matrix is situated between adjacent Tomes' processes of neighboring ameloblasts and results in the formation of the so-called "pits" (Fig. 4A, B). Pits surround the Tomes' process completely and can be up to 10 μm deep (Nanci et al. 1996). There is consensus in the literature that the pits of the secretory stage of amelogenesis will transform into the interrod enamel of the fully mineralized tissue, while the crystals that develop in matrices secreted through distTP will constitute the enamel rods (Nanci and Ten Cate 2013).

The most frequently used illustration of human enamel structure is based on the keyhole-like appearance of the enamel rods (Fig. 4C) (Meckel et al. 1965). This model is based on observations of pits with keyhole morphology (Fig. 4A) (Boyde 1967). There are also numerous studies, predominantly in rodents, which show pits with rectangular morphology or 4-fold symmetry (Nanci et al. 1985) (Fig. 4B). The 2 different pit morphologies, keyhole and rectangular, must be associated with 2 different morphologies of the Tomes' process. Finger-like protrusions will fit into the hollow structures of the rectangular pits (Fig. 4B), while Tomes' processes will adapt a keyhole morphology to match the keyhole structure of the pits (Skobe 2006). The ameloblast's mobility is restricted when the Tomes' process adapts a keyhole-like morphology due to the interlocking nature of the structure. This morphology is therefore dominant in areas without decussation. To allow cells to slide by each other laterally, the Tomes' process needs to adapt a different morphology. The finger-like appearance of the Tomes' process will produce the rectangular arrangement as shown in Fig. 4B. This morphology does allow for sliding in at least 2 directions and would enable decussating prisms to develop. Enamel that is heavily decussated, like the enamel in rodents, cows, goats, and, to some degree, in humans, is therefore composed predominantly of round enamel rods that derived from the finger-like Tomes' processes (Fig. 1E–J). The different pit patterns observed in these types of prismatic enamel also result in different types of interrod enamel. In decussating enamel, apatite nanofibers have a different

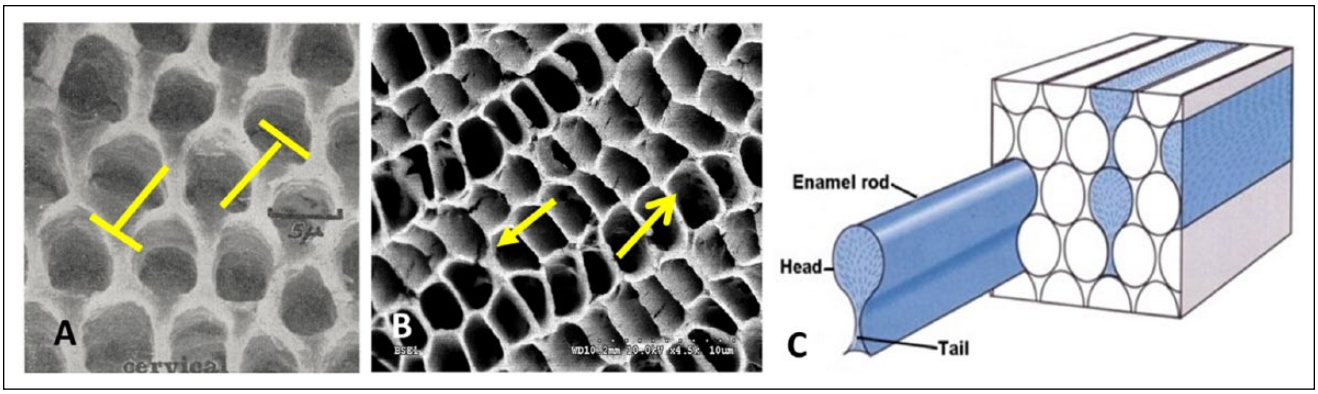

Figure 4. Relationship among the Tomes' process, the pits, and rod/interrod development in prismatic enamel. (**A**) Pits of Tomes' processes remain after removal of ameloblasts from secretory enamel and have a keyhole-like morphology that renders lateral movement of ameloblasts impossible (blocked arrows) (with permission from Boyde 1967). (**B**) Pits in secretory enamel from developing molar of a 5-d-old rodent show rectangular morphology, which allows for sliding movement of ameloblasts as indicated by arrows. (**C**) Classic schematic of the microstructure of human enamel composed of keyhole-like enamel rods (modified with permission from Meckel et al. 1965).

orientation in the interrod enamel compared with the enamel rods. This is clearly illustrated in the micrographs of bovine and goat enamel where the interrod enamel forms a continuous phase that intercepts the enamel rods (Fig. 1E, F). The enamel rods are not keyhole-like but are circular in this type of enamel. Circular rods also exist in human teeth (Fig. 1H) and are located in areas where rods decussate.

Both elements, rod decussation and the presence of interrod enamel, are linked to each other. Not only do both contribute to an increased toughness of enamel, but also they both derive from the same evolutionary origin, the development of a Tomes' process and the advent of prismatic enamel.

Possible Contributions of Matrix Proteins to Interrod Enamel

The significant contributions of structural elements to the mechanical behavior of enamel have been elucidated over the last 5 years. Recent advances in mechanical testing equipment and specimen preparation allowed for improved fracture toughness determination of small and notched enamel specimens (Ritchie et al. 2008; Bajaj and Arola 2009a, b; Bechtle, Fett, et al. 2010; Bechtle, Habelitz, et al. 2010). The results are different from those of earlier studies based on microindentation (White et al. 2001; Baldassarri et al. 2008). Analysis of these data showed toughness of human and bovine enamel to be significantly higher than previous measurements, with KI_c-values reaching 2–4 $MPam^{1/2}$. Studies also showed that resistance to crack propagation increased with crack extension, termed "R-curve behavior," substantiating that toughening elements do exist in enamel and are able to work against the advancement of cracks. In other words, cracks can become stable at a certain stress level. Additional energy or increased force is required to drive the crack through the material and to complete the fracture. Real-time crack propagation analysis showed that areas of decussating enamel rods induced deflection and bridging of the crack plane (Fig. 5A).

Many studies have shown that rod orientation and apatite fiber alignment in mammalian enamel are quite complex and far from similar to the aprismatic enamel of crocodiles (Fig. 1C, D). The zigzagged shape of a crack that develops from fracture through an area of enamel with a high degree of decussation demonstrates the difference the presence of enamel rods makes with regard to fracture resistance compared with the fracture of aprismatic enamel of reptiles (Yilmaz et al. 2014). Since decussated rods contribute to enamel toughening, the occurrence of interrod enamel also renders crack propagation more difficult. Since cracks tend to follow the long axes of apatite fibers, cracks deflect at the intersection of rod and interrod enamel. Fracture surfaces illustrate how a crack plane is deviated at the interrod enamel to follow the changing orientation of crystallites (Fig. 5B).

Interrod crystals are not different in size and shape from the crystals that run parallel in the enamel rod. Therefore, they may form by identical mechanisms of protein-guided crystallization. Interrod enamel, however, is laid down earlier as it develops in the matrix that constitutes the pits of the Tomes' processes. Electron microscopy of the prismatic enamel structure suggests that the orientation of apatite nanofibers depends on the location of secretion along the Tomes' process. Apatite ribbons align parallel to the rod axis in areas adjacent to the distal end of the Tomes' process, but that orientation differs when the apatite ribbons formed in the interrod enamel and in a matrix that was secreted by the proxTP. In both cases, the apatite fibers extend approximately perpendicular to the cell membrane. Since distal and proximal ends of the Tomes' process are oriented at an angle of about 30°, enamel crystallites in rod and interrod enamel also show this angulation.

Figure 5C illustrates schematically how the 2 distinct orientations of apatite ribbons could be achieved. Apatite ribbons connected to the proxTP will align in a different orientation than apatite ribbons associated with distTP. It is hypothesized in this illustration that enamel matrix proteins provide the link between apatite crystals and the cell membrane. The mechanisms by which the enamel matrix proteins control apatite

crystal morphology and orientation are not well-understood. When the stages of aprismatic reptile enamel are compared with those of prismatic mammalian enamel, it appears that ameloblasts developed a mechanism that allowed for connecting to a matrix that is able to produce fibrous apatite crystals. For cells to precisely direct the orientation of apatite nanofibers in rod and interrod enamel, the inorganic crystals are somehow connected to the cell membrane, or at least oriented by a textured matrix. Enamel protein most likely provides such a link. Both the ameloblastin and amelogenin genes contain domains that indicate an ability for lectin- and cell-binding (Ravindranath et al. 2000; Fukumoto et al. 2004).

Self-assembly of matrix proteins into a highly organized nanostructure will be required to generate the intricate architecture of enamel. Amelogenin is known to assemble into nanospheres and has shown a propensity for crystallization of needle-like apatite crystals (Moradian-Oldak 2012). However, in recent studies by our group, we have shown that amelogenin can also assemble into nanoribbons of 17 nm width (He et al. 2011; Martinez-Avila et al. 2011; Martinez-Avila et al. 2012). Such amelogenin ribbons self-align and mimic the oriented arrangement of apatite ribbons of the secretory stage of amelogenesis. They could therefore act as suitable templates for the generation of aligned apatite nanoribbons in enamel.

While amelogenin constitutes about 90% of the organic matter in secretory enamel, it was surprising to find that deletion of the amelogenin gene did not have as severe an effect on enamel as did the deletion of 2 other enamel proteins, e.g., enamelin and ameloblastin (Gibson et al. 2001; Smith et al. 2011). The Amelx$^{-/-}$ mouse produced a mineralized layer of various thicknesses between one-fourth and one-half of normal murine enamel. Its ultrastructure is aprismatic and composed of short apatite fibers with good parallel alignment (Fig. 1K, L) and thus is quite comparable with the primitive enamel of reptiles (Fig. 1C, D). Histologic analysis of incisors from these knockout animals suggests the lack of a long Tomes' process and migration of the ameloblast in parallel to the rod axis, without the angulation characteristic of the ameloblast layer in mammalian tissue (Espirito Santo et al. 2007). Amelogenin may therefore be critical for the development of enamel rods and interrods and for control over crystal alignment in these structural components. This hypothesis is also supported by a phylogenic analysis that showed that amelogenin is derived from ameloblastin and is evolutionarily the youngest among the 3 main components of secretory enamel proteins (Delgado et al. 2008; Assaraf-Weill et al. 2013). The formation of an extended

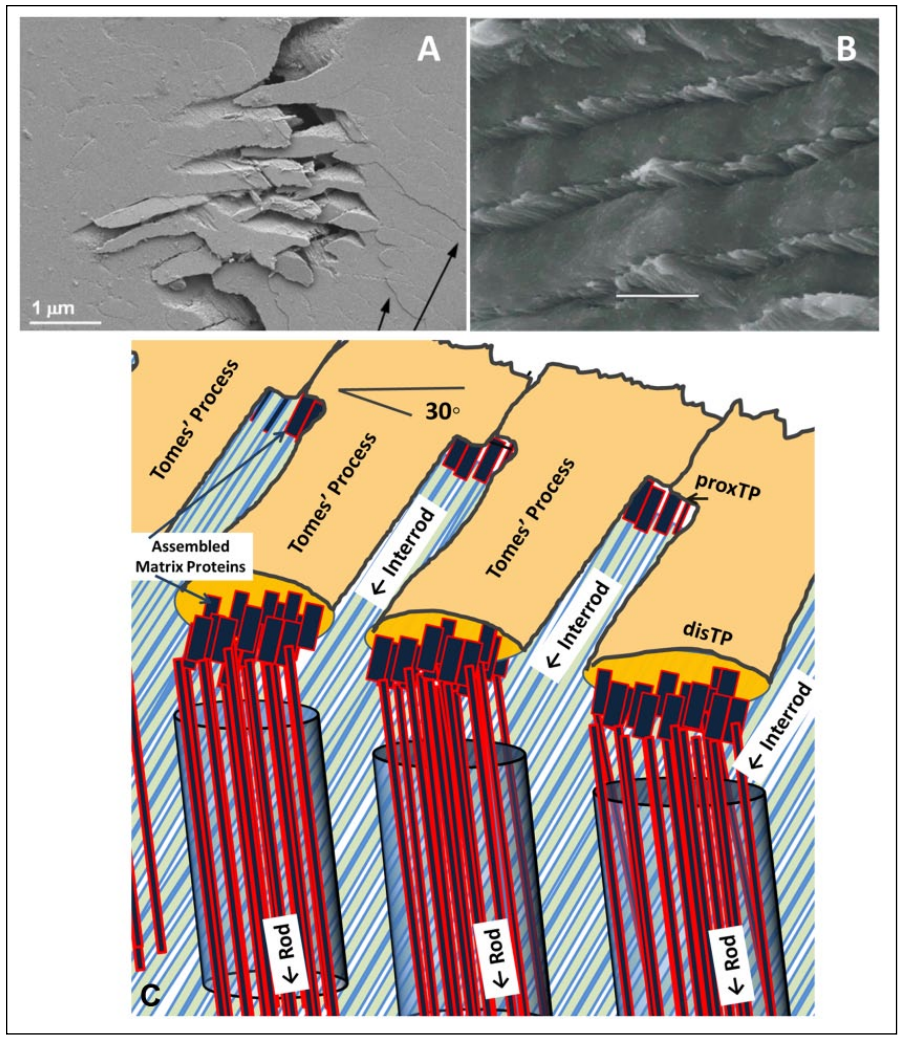

Figure 5. Improved fracture resistance in mammalian enamel is a consequence of ameloblast's ability to control apatite fiber orientation in rod and interrod enamel. (**A, B**) Scanning electron microscope micrographs of fracture planes through human dental enamel. (A) Crack propagating along enamel rods is heavily deviated in the area of decussation, creating a zigzag pattern. Arrows point to microcracks growing perpendicular to the fracture plane (image courtesy of S. Bechtle, TU Hamburg-Harburg, Germany). (B) Fracture surface of human enamel illustrating the toughening capacity of the interrod rod enamel as it causes the growing crack to deviate from its straight path through the enamel. (**C**) Schematic illustrating a possible mechanism for achieving different orientations of apatite fibers in enamel rods vs interrod enamel. Initial apatite ribbons in both rod and interrod enamel are only 2–3 nm thick and 10–20 nm wide. Difference in orientation is achieved by secretion at 2 different sites of the Tomes' process. Apatite ribbons that form in matrices secreted through the distal end (distTP) are parallel to the rod axis, while mineral ribbons that formed in matrices secreted through the proximal end of the Tomes' process (proxTP) align in an angle to the direction of the enamel rod. Ribbons most likely attach to cell membrane through assembled protein structure or are guided by an organized matrix structure to achieve control over mineral fiber orientation. The model allows for continuity of interrod crystals throughout enamel as a fibrous continuum described in the literature (White et al. 2001).

Tomes' process and the development of prismatic enamel may therefore be intertwined with the evolution of the amelogenin gene.

Conclusions

Evolution of ameloblast gene products, changes in cell morphology, and secretion of matrix proteins have optimized the enamel structure, predominantly to improve its longevity. From an initially hard, nanofibrous apatite tissue with significant fiber alignment but low fracture tolerance, enamel evolved into a complex architecture of domains of parallel apatite nanofibers, which decussate at oblique angles between enamel rods and between rod and interrod enamel. Furthermore, the presence of a stiffness gradient across the thickness of enamel helps to integrate the stiff enamel with underlying softer dentin by reducing stresses at the DEJ. The structural engineering of enamel is the achievement of ameloblasts and its evolution. Our understanding of the molecular mechanisms and the developmental biology of ameloblasts will benefit from an inclusion of structural engineering and functional concepts of enamel to the discussion of processes in amelogenesis.

Author Contributions

S. Habelitz, contributed to conception, design, and data acquisition, drafted and critically revised the manuscript. The author gave final approval and agrees to be accountable for all aspects of the work.

Acknowledgments

Specimens for SEM analysis of enamel structure in the shark, crocodile, and goat were provided by Dr. Thomas Diekwisch (UIC). Dr. Megan Pugach (Forsyth Institute) provided tissue specimens of Amelx$^{-/-}$ mice. Drs. Gerold Schneider (TU Hamburg-Harburg) and Antonio Nanci (Montreal) contributed insights into fracture mechanics and enamel structure. Melissa Milder (UCSF) assisted with SEM specimen preparation. The research was supported by National Institutes of Health (NIH)/National Institute of Dental and Craniofacial Research (NIDCR) DE023422. The authors declare no potential conflicts of interest with respect to the authorship and/or publication of this article.

References

Assaraf-Weill N, Gasse B, Al-Hashimi N, Delgado S, Sire JY, Davit-Beal T. 2013. Conservation of amelogenin gene expression during tetrapod evolution. J Exp Zool B Mol Dev Evol. 320(4):200–209.

Assaraf-Weill N, Gasse B, Silvent J, Bardet C, Sire JY, Davit-Beal T. 2014. Ameloblasts express type I collagen during amelogenesis. J Dent Res. 93(5):502–507.

Bajaj D, Arola D. 2009a. Role of prism decussation on fatigue crack growth and fracture of human enamel. Acta Biomater. 5(8):3045–3056.

Bajaj D, Arola DD. 2009b. On the R-curve behavior of human tooth enamel. Biomaterials. 30(23-24):4037–4046.

Baldassarri M, Margolis HC, Beniash E. 2008. Compositional determinants of mechanical properties of enamel. J Dent Res. 87(7):645–649.

Bartlett JD, Ganss B, Goldberg M, Moradian-Oldak J, Paine ML, Snead ML, Wen X, White SN, Zhou YL. 2006. 3. Protein-protein interactions of the developing enamel matrix. Curr Top Dev Biol. 74:57–115.

Bechtle S, Fett T, Rizzi G, Habelitz S, Schneider GA. 2010. Mixed-mode stress intensity factors for kink cracks with finite kink length loaded in tension and bending: application to dentin and enamel. J Mech Behav Biomed Mater. 3(4):303–312.

Bechtle S, Habelitz S, Klocke A, Fett T, Schneider GA. 2010. The fracture behaviour of dental enamel. Biomaterials. 31(2):375–384.

Boyde A. 1967. The development of enamel structure. Proc R Soc Med. 60(9):923–928.

Chang CC, Hsu IK, Aykol M, Hung WH, Chen CC, Cronin SB. 2010. A new lower limit for the ultimate breaking strain of carbon nanotubes. ACS Nano. 4(9):5095–5100.

Currey JD. 2002. Bones: structure and mechanics. Princeton, NJ: Princeton University Press.

Cuy JL, Mann AB, Livi KJ, Teaford MF, Weihs TP. 2002. Nanoindentation mapping of the mechanical properties of human molar tooth enamel. Arch Oral Biol. 47(4):281–291.

Daculsi G, Kerebel B. 1978. High-resolution electron-microscope study of human enamel crystallites - size, shape, and growth. J Ultra Mol Struct R. 65(2):163–172.

Davit-Beal T, Allizard F, Sire JY. 2007. Enameloid/enamel transition through successive tooth replacements in *Pleurodeles waltl* (Lissamphibia, Caudata). Cell Tissue Res. 328(1):167–183.

Delgado S, Vidal N, Veron G, Sire JY. 2008. Amelogenin, the major protein of tooth enamel: a new phylogenetic marker for ordinal mammal relationships. Mol Phylogenet Evol. 47(2):865–869.

Diekwisch TG, Berman BJ, Anderton X, Gurinsky B, Ortega AJ, Satchell PG, Williams M, Arumugham C, Luan X, McIntosh JE, et al. 2002. Membranes, minerals, and proteins of developing vertebrate enamel. Microsc Res Tech. 59(5):373–395.

Diekwisch TG, Jin T, Wang X, Ito Y, Schmidt M, Druzinsky R, Yamane A, Luan X. 2009. Amelogenin evolution and tetrapod enamel structure. Front Oral Biol. 13:74–79.

Enax J, Fabritius HO, Rack A, Prymak O, Raabe D, Epple M. 2013. Characterization of crocodile teeth: correlation of composition, microstructure, and hardness. J Struct Biol. 184(2):155–163.

Espirito Santo AR, Bartlett JD, Gibson CW, Li Y, Kulkarni AB, Line SR. 2007. Amelogenin- and enamelysin (Mmp-20)-deficient mice display altered birefringence in the secretory-stage enamel organic extracellular matrix. Connect Tissue Res. 48(1):39–45.

Feng L, Chittenden M, Schirer J, Dickinson M, Jasiuk I. 2012. Mechanical properties of porcine femoral cortical bone measured by nanoindentation. J Biomech. 45(10):1775–1782.

Fraser GJ, Cerny R, Soukup V, Bronner-Fraser M, Streelman JT. 2010. The odontode explosion: the origin of tooth-like structures in vertebrates. Bioessays. 32(9):808–817.

Fratzl P. 2008. Collagen: structure and mechanics. New York: Springer.

Fukumoto S, Kiba T, Hall B, Iehara N, Nakamura T, Longenecker G, Krebsbach PH, Nanci A, Kulkarni AB, Yamada Y. 2004. Ameloblastin is a cell adhesion molecule required for maintaining the differentiation state of ameloblasts. J Cell Biol. 167(5):973–983.

Gibson CW, Yuan ZA, Hall B, Longenecker G, Chen E, Thyagarajan T, Sreenath T, Wright JT, Decker S, Piddington R, et al. 2001. Amelogenin-deficient mice display an amelogenesis imperfecta phenotype. J Biol Chem. 276(34):31871–31875.

Gillis JA, Donoghue PC. 2007. The homology and phylogeny of chondrichthyan tooth enameloid. J Morphol. 268(1):33–49.

Griffith AA. 1921. Phenomena of rupture and flow in solids. Philos T R Soc A. 221:163–198.

Habelitz S, Marshall SJ, Marshall GW Jr, Balooch M. 2001. Mechanical properties of human dental enamel on the nanometre scale. Arch Oral Biol. 46(2):173–183.

Hanaizumi Y, Shimokobe H, Wakita M. 1994. The three-dimensional structure of Tomes' processes and their relationship to arrangement of enamel prism in dog teeth. Arch Histol Cytol. 57(2):129–138.

He LH, Swain MV. 2009. Enamel—a functionally graded natural coating. J Dent. 37(8):596–603.

He XD, Wu SP, Martinez-Avila O, Cheng YF, Habelitz S. 2011. Self-aligning amelogenin nanoribbons in oil-water system. J Struct Biol. 174(1):203–212.

Imbeni V, Kruzic JJ, Marshall GW, Marshall SJ, Ritchie RO. 2005. The dentin-enamel junction and the fracture of human teeth. Nat Mater. 4(3):229–232.

Jeng YR, Lin TT, Hsu HM, Chang HJ, Shieh DB. 2011. Human enamel rod presents anisotropic nanotribological properties. J Mech Behav Biomed Mater. 4(4):515–522.

Katz JL, Ukraincik K. 1971. On the anisotropic elastic properties of hydroxyapatite. J Biomech 4(3):221–227.

Kinney JH, Marshall SJ, Marshall GW. 2003. The mechanical properties of human dentin: a critical review and re-evaluation of the dental literature. Crit Rev Oral Biol Med. 14(1):13–29.

Lawn BR, Deng Y, Lloyd IK, Janal MN, Rekow ED, Thompson VP. 2002. Materials design of ceramic-based layer structures for crowns. J Dent Res. 81(6):433–438.

Lyaruu DM, Medina JF, Sarvide S, Bervoets TJ, Everts V, Denbesten P, Smith CE, Bronckers AL. 2014. Barrier formation: potential molecular mechanism of enamel fluorosis. J Dent Res. 93(1):96–102.

Mann S. 2001. Biomineralization, principles and concepts in bioinorganic materials chemistry. Oxford, UK: Oxford University Press.

Marshall GW, Habelitz S, Gallagher R, Balooch M, Balooch G, Marshall SJ. 2001. Nanomechanical properties of hydrated carious human dentin. J Dent Res. 80(8):1768–1771.

Martinez-Avila OM, Wu S, Cheng Y, Lee R, Khan F, Habelitz S. 2011. Self-assembly of amelogenin proteins at the water-oil interface. Eur J Oral Sci. 119(Suppl 1):75–82.

Martinez-Avila O, Wu S, Kim SJ, Cheng Y, Khan F, Samudrala R, Sali A, Horst JA, Habelitz S. 2012. Self-assembly of filamentous amelogenin requires calcium and phosphate: from dimers via nanoribbons to fibrils. Biomacromolecules. 13(11):3494–3502.

Meckel AH, Griebstein WJ, Neal RJ. 1965. Structure of mature human dental enamel as observed by electron microscopy. Arch Oral Biol. 10(5):775–783.

Meyers MA, Chen PY, Lopez MI, Seki Y, Lin AY. 2011. Biological materials: a materials science approach. J Mech Behav Biomed Mater. 4(5):626–657.

Moradian-Oldak J. 2012. Protein-mediated enamel mineralization. Front Biosci. 17:1996–2023.

Nalla RK, Kruzic JJ, Kinney JH, Ritchie RO. 2005. Mechanistic aspects of fracture and R-curve behavior in human cortical bone. Biomaterials. 26(2):217–231.

Nanci A, Bendayan M, Slavkin HC. 1985. Enamel protein biosynthesis and secretion in mouse incisor secretory ameloblasts as revealed by high-resolution immunocytochemistry. J Histochem Cytochem. 33(11):1153–1160.

Nanci A, Hashimoto J, Zalzal S, Smith CE. 1996. Transient accumulation of proteins at interrod and rod enamel growth sites. Adv Dent Res. 10(2):135–149.

Nanci A, Ten Cate AR. 2013. Ten Cate's oral histology: development, structure, and function. 8th ed. St. Louis, MO: Elsevier.

Ravindranath RM, Tam WY, Nguyen P, Fincham AG. 2000. The enamel protein amelogenin binds to the N-acetyl-D-glucosamine-mimicking peptide motif of cytokeratins. J Biol Chem. 275(50):39654–39661.

Ritchie RO, Koester KJ, Ionova S, Yao W, Lane NE, Ager JW 3rd. 2008. Measurement of the toughness of bone: a tutorial with special reference to small animal studies. Bone. 43(5):798–812.

Sa Y, Liang S, Ma X, Lu S, Wang Z, Jiang T, et al. 2014. Compositional, structural and mechanical comparisons of normal enamel and hypomaturation enamel. Acta Biomater. 10(12):5169–5177.

Sahni A. 1987. Evolutionary aspects of reptilian and mammalian enamel structure. Scanning Microsc. 1(4):1903–1912.

Sander PM. 2000. Prismless enamel in amniotes: terminology, function and evolution. In: Teaford MF, Smith MM, Ferguson MWJ, editors. Development, function and evolution of teeth. Cambridge: Cambridge University Press. p. 92–106.

Sasagawa I, Ishiyama M, Yokosuka H, Mikami M, Uchida T. 2009. Tooth enamel and enameloid in actinopterygian fish. Front Mater Sci. 3(2):174–182.

Satchell PG, Anderton X, Ryu OH, Luan X, Ortega AJ, Opamen R, Berman BJ, Witherspoon DE, Gutmann JL, Yamane A, et al. 2002. Conservation and variation in enamel protein distribution during vertebrate tooth development. J Exp Zool. 294(2):91–106.

Simmer JP, Hu JC. 2002. Expression, structure, and function of enamel proteinases. Connect Tissue Res. 43(2-3):441–449.

Simmer JP, Papagerakis P, Smith CE, Fisher DC, Rountrey AN, Zheng L, Hu JC. 2010. Regulation of dental enamel shape and hardness. J Dent Res. 89(10):1024–1038.

Skobe Z. 2006. SEM evidence that one ameloblast secretes one keyhole-shaped enamel rod in monkey teeth. Eur J Oral Sci. 114(Suppl 1):338–342.

Smith CE, Hu Y, Richardson AS, Bartlett JD, Hu JC, Simmer JP. 2011. Relationships between protein and mineral during enamel development in normal and genetically altered mice. Eur J Oral Sci. 119(Suppl 1):125–135.

Smith MM, Coates MI. 1998. Evolutionary origins of the vertebrate dentition: phylogenetic patterns and developmental evolution. Eur J Oral Sci. 106(Suppl 1):482–500.

Soukup V, Epperlein HH, Horacek I, Cerny R. 2008. Dual epithelial origin of vertebrate oral teeth. Nature. 455(7214):795–798.

Thesleff I, Hurmerinta K. 1981. Tissue interactions in tooth development. Differentiation. 18(2):75–88.

Tye CE, Pham CT, Simmer JP, Bartlett JD. 2009. DPPI may activate KLK4 during enamel formation. J Dent Res. 88(4):323–327.

White SN, Luo W, Paine ML, Fong H, Sarikaya M, Snead ML. 2001. Biological organization of hydroxyapatite crystallites into a fibrous continuum toughens and controls anisotropy in human enamel. J Dent Res. 80(1):321–326.

Whitenack LB, Simkins DC Jr, Motta PJ, Hirai M, Kumar A. 2010. Young's modulus and hardness of shark tooth biomaterials. Arch Oral Biol. 55(3):203–209.

Wong FS, Anderson P, Fan H, Davis GR. 2004. X-ray microtomographic study of mineral concentration distribution in deciduous enamel. Arch Oral Biol. 49(11):937–944.

Yilmaz ED, Bechtle S, Ozcoban H, Kieser JA, Swain MV, Schneider GA. 2014. Micromechanical characterization of prismless enamel in the tuatara, *Sphenodon punctatus*. J Mech Behav Biomed Mater. 39:210–217.

Zheng L, Hilton JF, Habelitz S, Marshall SJ, Marshall GW. 2003. Dentin caries activity status related to hardness and elasticity. Eur J Oral Sci. 111(3):243–252.